

Spatially Indirect Exciton Condensation in Two-Dimensional Strongly Correlated Semimetals

Yao Zeng, Shi-Cong Mo, and Wéi Wú*

School of Physics, Sun Yat-sen University, Guangzhou, Guangdong 510275, China

(Dated: March 20, 2026)

Identifying materials hosting an excitonic insulator ground state has been one of the major pursuits in condensed matter physics in recent years. Promising candidates in transition metal chalcogenide compounds (TMC), including $1T - \text{TiSe}_2$, $\text{Ta}_2\text{Pd}_3\text{Te}_5$, and Ta_2NiSe_5 , share a crucial common characteristic: their low-energy physics is governed by electrons in $d-$ orbitals subject to strong on-site Coulomb interactions. In this work, we investigate spatially indirect exciton condensation in two-dimensional semimetals on triangular lattice. Using a combination of dynamical mean-field theory and the determinant quantum Monte Carlo method, we study two- and three-orbital Hubbard models incorporating strong on-site (U) and inter-orbital interactions (V). Our results demonstrate that on-site Hubbard U can strongly suppress the condensation temperature T_c , an effect that is particularly pronounced at higher electron-hole pair densities. This behavior contrasts sharply with the case without on-site U , where T_c grows with pair density at fixed V . Moreover, we uncover competition among multiple electron-hole pairing channels in the three-orbital model, which also acts to suppress T_c of exciton condensation. An orbital-selective electron-hole pairing state is identified. These findings may help explain the large discrepancy between strong binding-energy and relative low transition temperature for indirect excitons in TMCs materials, offering important insights for understanding and engineering exciton condensation in materials with strongly correlated $d-$ shell electrons.

Introduction- The excitonic insulator (EI) constitutes a paradigmatic correlated state arising from a bosonic condensation of Coulomb-bound electron-hole pairs in narrow-gap semiconductors or semimetals [1–4]. This fundamental phase of matter has been investigated extensively in both experiment [5–13] and theory [2, 3, 6, 14–21]. The spatially separated electron-hole bilayer structures [4] provide particularly favorable platforms for achieving this state, as spatial separation suppresses electron-hole recombination, hence prolonging exciton lifetimes and promotes the condensation of indirect excitons. The exploration of many exotic emergent phenomena related to EI, such as the BCS-BEC crossover [22–30], supersolidity [31–33], finite momentum pairing [34–37], excitonic topological phases [11, 38], and perfect Coulomb Drag [39, 40], can thus be facilitated in the indirect exciton systems.

Quantum wells in InAs/GaSb heterostructures have served as pioneering platforms in the pursuit of these exotic phases [38, 41]. These semiconductor systems revealed signatures of excitonic topological order and superfluidity [4, 38, 42]. More recently, transition metal chalcogenide (TMC) platforms, such as $\text{MoSe}_2/\text{hBN}/\text{WSe}_2$ heterostructures, have been pivotal systems for hosting high-temperature EI [39, 40]. By exploiting Type-II band alignment to spatially separate carriers, these devices host long-lived excitons that exhibit macroscopic coherence, evidenced by nonlinear electroluminescence up to 100 K [30]. Crucially, transport measurements revealed perfect Coulomb drag at zero magnetic field [39, 40], establishing a key foundation for enabling frictionless flow of charge-neutral excitons [43–46] in transport experiments. In bulk EI ma-

terials, on the other hand, the layered TMC compounds $1T - \text{TiSe}_2$ [5, 47, 48], $\text{Ta}_2\text{Pd}_3\text{Te}_5$ [9, 10], and Ta_2NiSe_5 [9, 10, 19, 49, 50] have sparked intense debate regarding the existence of exciton condensation. This is because the gap opening in these materials, a hallmark of the excitonic ordered state, can also be attributed to non-excitonic structure phase transitions [8, 51–54]. Compared to Ta_2NiSe_5 , which may host significant structural distortion [53, 55], $\text{Ta}_2\text{Pd}_3\text{Te}_5$ offers a cleaner paradigm, as in which the lattice distortion is negligible in the insulating phase [9, 10]. This structural stability strongly supports an exciton instability driven by Coulomb interactions in $\text{Ta}_2\text{Pd}_3\text{Te}_5$.

While experimental advances in the study of EI have progressed rapidly, a comprehensive theoretical understanding [15, 22, 33, 56–60] of this phase in real materials remains incomplete. We notice that in theory, large exciton binding energies being order of $\sim 1\text{eV}$ have been predicted in semi-metals or narrow gap semiconductors [19, 61–63], a high temperature EI in experiments, however, is still elusive. Conventional theoretical frameworks are often established on the basis of mean-field or perturbative approaches. In EI candidate materials based on TMC, the strong on-site Hubbard interaction U in $d-$ orbitals is usually larger than the electron bandwidth W [64], and it can significantly exceed the inter-orbital (inter-layer) electron-hole attraction V [51]. This strong-correlation regime calls into question the adequacy of weak-coupling theories that consider V while neglecting the substantial on-site interaction U .

In this work, we investigate excitonic condensation in two-dimensional (2D) semimetals using a combination of Cellular dynamical Mean-Field theory (CDMFT) [65]

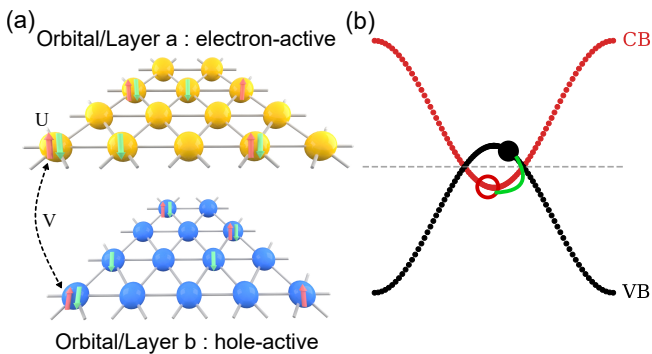


FIG. 1. (a) Schematic illustration of the two-orbital (two-layer) Hubbard model on 2D triangular lattice. U represents the on-site intra-orbital(intra-layer) Coulomb interaction, while V denotes the inter-orbital (inter-layer) Coulomb interaction in a unit cell. The orbital/layer a (upper) is designated as electron-active, while orbital/layer b (lower) acts as hole-active. Dotted line indicates a possible electron-hole pairing. (b) Schematic illustration of the non-interacting band structure we use which is a semimetal at $U = 0, V = 0$. Red (black) curves indicate the conduction (valence) bands. The pairing of holes at the CB bottom (red hollow circles) and electrons at the VB top (black filled circles) leads to the formation of indirect excitons. Dashed line indicates Fermi level.

and determinant quantum Monte Carlo (DQMC) [66]. The non-perturbative CDMFT approach enables us to capture the quantum fluctuation of strongly interacting d -electrons beyond weak-coupling treatments. We show that the excitonic condensation temperature T_c can be significantly suppressed by on-site Coulomb repulsion U , although it in general remains non-zero for finite V . We also show that a finite U fundamentally modifies the density dependence of T_c . Specifically, T_c drops with increasing carrier concentration n , which contrasts with the $U = 0$ case, where T_c grows with pair density n at fixed V . Using a three-orbital model, we further uncover the competition between different pairing channels, which provides an additional mechanism suppressing T_c . An orbital-selective EI state is also revealed in this model. Finally, we discuss the implications of these findings for experimental observations.

Model and Methods - Our two-orbital Hubbard model we use is given by,

$$H = - \sum_{\langle ij \rangle \sigma m} t_m c_{i\sigma m}^\dagger c_{j\sigma m} + \text{H.c.} - \sum_{i\sigma m} (\mu - \epsilon_m) \hat{n}_{i\sigma m} + \sum_{im} U_m \hat{n}_{i\uparrow m} \hat{n}_{i\downarrow m} + V \sum_{i\sigma\sigma', m \neq m'} \hat{n}_{i\sigma m} \hat{n}_{i\sigma' m'} \quad (1)$$

where the $m = a, b$ labels the orbital (or layer) degrees of freedom, corresponding to orbitals in bulk systems and layers in 2D materials, respectively. $c_{i\sigma m}$ ($c_{i\sigma m}^\dagger$) denotes the electron annihilation (creation) operator at unit cell i , orbital (layer) m , with spin σ ; $n_{i\sigma m}$ is the particle

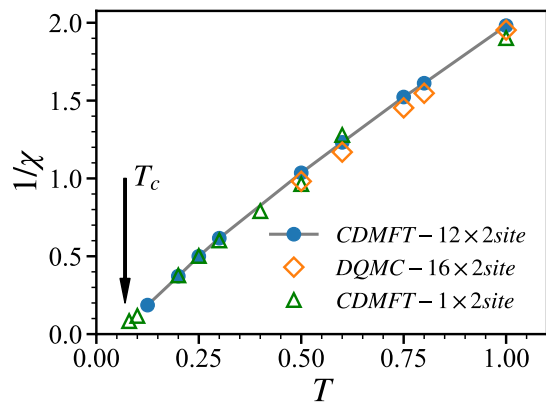


FIG. 2. The inverse susceptibility $1/\chi$ as a function of temperature T . When $1/\chi$ approaches zero, the system enters the excitonic condensate phase, and the corresponding temperature is defined as the critical transition temperature T_c . Here, $U_a = U_b = 1, V = 4$, density, $\langle n_a \rangle = 0.2, \langle n_b \rangle = 0.8$ (thus $n_e = n_h = 0.2$). An excitonic condensation T_c is found about $T_c \sim 0.07$. The DQMC calculations were performed on a $4 \times 4 \times 2$ lattice, while DMFT calculations were performed on 1×2 - and 12×2 -site clusters.

number operator. The nearest-neighbor hopping integral t_a is set to $t_a = t = 1$ as energy unit throughout the paper. U_m is the on-site repulsion between electrons at orbital (layer) $-m$, V is the local inter-orbital (inter-layer) interaction. In this work, we have omitted long-range Coulomb interactions to simplify the numerical study. We adjust chemical potential μ and orbital(layer) energy ϵ_m to tune the orbital (layer) densities. Here we adopt a pure electron picture to study the problem, *i.e.*, $\langle \hat{n}_a \rangle = n_e \equiv n$ denote the carrier density in the electron orbital (orbital- a), implying a hole orbital (layer) of $n_h = 1 - \langle \hat{n}_b \rangle = n_e = n$ in the orbital- b . We assume equal mass for both carriers, *i.e.*, $t_a = -t_b$. The schematic of our model and the simplified semimetal band structure are illustrated in Fig. 1. Orbitals (layers) a (upper) and b (lower) are designated as electron-active and hole-active, respectively.

Our theoretical investigation of the bilayer Hubbard model on a triangular lattice is carried out by the Cellular Dynamical Mean-Field Theory, a cluster extension of DMFT [65] designed to incorporate non-local spatial correlations. In this framework, the lattice problem is mapped onto an effective quantum impurity model for a small cluster, which is then solved self-consistently within a dynamical bath that represents the rest of the lattice degrees of freedom. Here we typically use a two-site effective cluster incorporating a, b orbitals within a unit cell. The effective cluster problem is solved using the continuous-time quantum Monte Carlo method (CTQMC)[67, 68]. Our simulations typically accumulate 10^9 Monte Carlo sweeps in each DMFT loop.

Result - The onset of the excitonic condensation phase can be identified by the divergence of the uniform exci-

tonic pairing susceptibility χ , which can be defined as,

$$\chi = \frac{1}{N} \sum_{i,j} \int_0^\beta d\tau \langle T_\tau p_j(\tau) p_i(0) \rangle \quad (2)$$

where p_i is the uniform spin-singlet electron-hole pair operator [23], $p_i = \frac{1}{\sqrt{2}} \sum_\sigma \langle c_{ia\sigma}^\dagger c_{ib\sigma} \rangle$, and N is the number of unit cells in the system. Thus the vanishing inverse pairing susceptibility $1/\chi \rightarrow 0$ can be used to determine the critical transition temperature T_c for excitonic condensation (i.e., T_c for EI). As shown in Fig. 2, we plot the CDMFT result of $1/\chi$ as a function of temperature T for a typical parameter set: $U_a = U_b = 1$, $V = 4$, and electron-hole density $n = 0.2$. As the temperature decreases from $T = 1.0$ to $T = 0.08$, $1/\chi$ drops monotonically from $1/\chi \approx 2.0$ to $1/\chi \approx 0$, signaling a growing tendency to EI condensation as T reduces. As T approaches $T_c \approx 0.07$, $1/\chi$ vanishes, denoting an EI instability in the system at the given parameters. We observe excellent agreement of 1×2 - and 12×2 - site CDMFT with exact high- T DQMC results on a $4 \times 4 \times 2$ - site lattice, thereby justifying the use of CDMFT to reliably capture the exciton physics.

We now focus on the dependence of critical temperature T_c on the inter-orbital electron-hole attraction V . In Fig. 3, results of T_c as a function of V are shown. The calculations are performed at a fixed electron-hole density $n = 0.06$, and two on-site repulsion $U = 0, U = 4$. In the absence of on-site repulsion ($U = 0$), T_c increases from $T_c \approx 0.006$ to $T_c \approx 0.12$ as V is increased from $V = 3$ to $V = 5$. For the finite U case ($U = 4$), T_c grows from $T_c \approx 0.012$ to $T_c \approx 0.1$ as V increases from $V = 4$ to

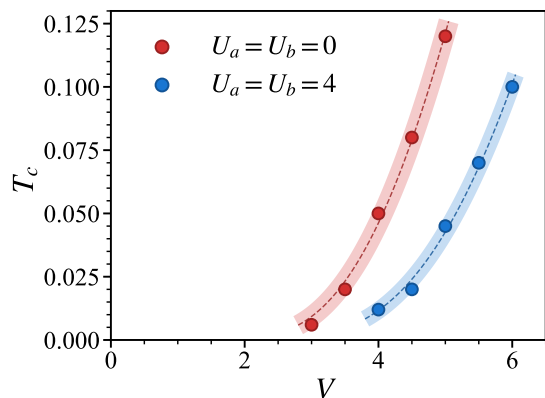


FIG. 3. Transition temperature T_c as a function of the inter-orbital interaction V for different values of the on-site interaction $U_a = U_b \equiv U$. Here, electron-hole density is fixed at $n_e = n_h = 0.06$, the data points represent results for $U = 0$ (red circles) and $U = 4$ (blue circles). The dashed lines depict fits to the BCS scaling trend, $T_c = Ae^{-B/V}$, while shaded ribbons indicate the corresponding confidence intervals. The extracted fitting parameters are $A \approx 5.73$, $B \approx 19.28$ for the non-interacting case ($U = 0$) and $A \approx 7.59$, $B \approx 25.90$ for the interacting case ($U = 4$).

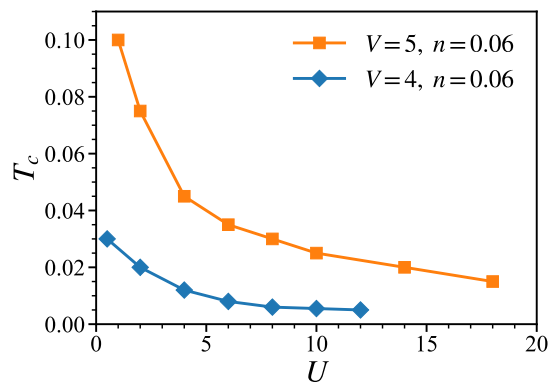


FIG. 4. Transition temperature T_c as a function of the on-site Coulomb interaction U at different values of inter-orbital interaction V . Orange symbols correspond to $V = 5$, while blue symbols correspond to $V = 4$. Here $n_e = n_h = n = 0.06$. 1×2 - site CDMFT is used here.

$V = 6$. At given V , T_c is consistently smaller for $U = 4$ than for $U = 0$, indicating on-site U plays a detrimental role in exciton condensation. For both curves, we find a trend qualitatively consistent with a BCS-like behavior is followed, $T_c \propto \exp(-B/V)$, namely, T_c are very small for $V < 3$, then grows rapidly, exhibiting an exponential-like rise as $V \geq 3$.

To investigate the effect of on-site Hubbard repulsion U on excitonic condensation in detail, we computed T_c across a wide range of U values. As shown in FIG. 4, T_c decreases substantially as U increases from zero, demonstrating a strong suppression of excitonic condensation by U . This decreasing trend is particularly rapid at smaller U and becomes more gradual for larger U , see both curves in FIG. 4. Specifically, at fixed $V = 5$, increasing U from $U = 1$ to $U = 18$ reduces T_c from $T_c = 0.1$ to $T_c = 0.015$, a decrease by nearly a factor of seven. Similarly, for $V = 4$, raising U from $U = 0.5$ to $U = 12$ lowers T_c from $T_c = 0.03$ to $T_c = 0.005$, corresponding to a sixfold reduction. These results confirm that the on-site repulsion U is a key factor limiting the stability of the excitonic condensed phase in the system.

Now we investigate the interplay between the on-site repulsion U and the electron-hole density. The density dependence of T_c for both $U = 0$ and $U = 8$ cases is shown in FIG 5. For the $U = 0$ case ($U = 0, V = 5$), T_c exhibits a monotonic increase from $T_c = 0.035$ to $T_c = 0.15$ as the density rises from $n = 0.005$ to $n = 0.08$, indicating that a larger population of charge carriers favours condensation. In stark contrast, the on-site repulsion fundamentally alters this behavior. In the low-density regime ($0.005 < n < 0.01$), T_c shows an initial increase for the $U = 8, V = 5$ case (diamonds in FIG. 5), rising from $T_c = 0.03$ to $T_c = 0.04$. However, as the density increases beyond $n = 0.01$, T_c begins to decrease continuously, dropping significantly from $T_c = 0.04$ to $T_c = 0.015$ as n increased from $n = 0.01$ to $n = 0.08$.

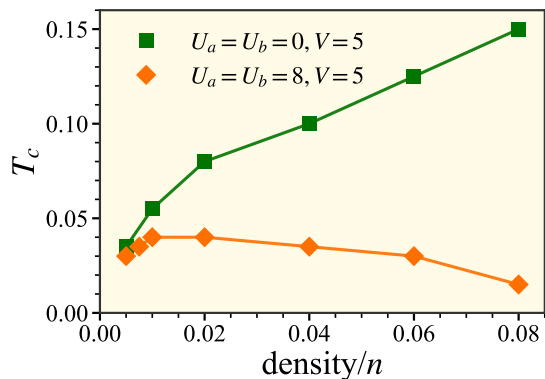


FIG. 5. Transition temperature T_c as a function of the electron-hole density at different values of the on-site interaction U . The inter-orbital interaction is fixed at $V = 5$, while the intra-orbital interaction is set to $U = 0$ (green line) and $U = 8$ (orange line). 1×2 - site CDMFT is used here.

This non-monotonic trend at finite U demonstrates a competition of mechanisms: for extremely low carrier density n , the on-site repulsion U is less important, increasing n enhances the coherence of electron-hole pairs, hence resulting in a higher T_c . When n becomes significantly large, the on-site repulsion tends to bind intra-orbital local electron-hole pairs, which competes with the formation of inter-orbital excitons, leading to a decreased T_c .

In essence, these results show that in a system where low-energy physics is dominated by d - electrons, the formation of indirect excitons faces significant competition from intra-orbital electron-hole binding. Consequently, the system's low-energy physics is not governed purely by inter-orbital (or inter-layer) excitonic degrees of freedom. A theoretical approach that consider only inter-orbital electron-hole binding may therefore miss a key physical ingredient and severely overestimate the phase transition temperature T_c .

Above we have studied the two-orbital electron-hole model. In materials, carriers near Fermi level can also originate from multiple d -orbitals, or from a hybridization with p -orbitals (which possess a smaller on-site U). For instance, in $\text{Ta}_2\text{Pd}_3\text{Te}_5$ [19], hole bands acquire weight from both the Pd- d_{xy} -orbital and Te- p_x -orbital. In Ta_2NiSe_5 , multiple Ta and Ni d -orbitals contribute to the relevant electron and hole bands [69]. This multiplicity of active orbitals can potentially give rise to several distinct channels for electron-hole pair condensation [51], which may compete with one another. To explore the interplay between multiple pairing channels involving d - or p -orbital degrees of freedom, we extend our analysis to a minimal three-orbital model [70–72]. Without loss of generality, we consider a system comprising one electron-type orbital (orbital- a) and two hole-type orbitals (orbital- b,c). In this system, an electron can, in principle, form a bound pair with a hole from either

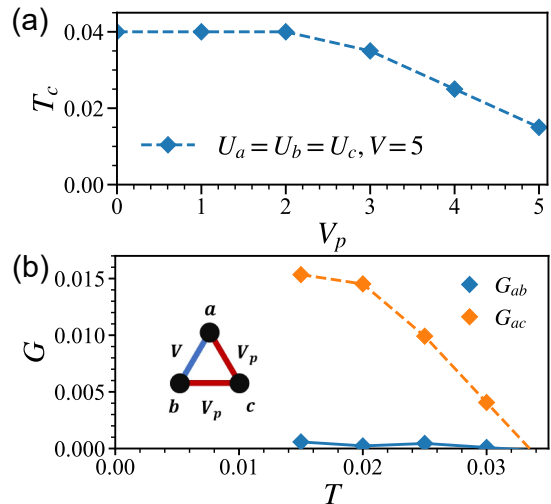


FIG. 6. (a) Transition temperature T_c as a function of inter-orbital d - d Coulomb interaction V_p . The parameters are set to electron-hole density $n = 0.06$, on-site Coulomb interactions $U_a = U_b = U_c = 4$, and inter- d -orbital interaction $V = 5$. (b) **Main panel:** Temperature dependence of the inter-orbital excitonic condensation order parameter G_{ab} (blue line) and G_{ac} (orange line) in the three-orbital model. Lines are guides for the eye. **Inset (left):** Schematic of the three-orbital model, where the a , b , c are distinct orbital indices. The additional orbital c represents the p -orbital, while a and b represent the d -orbitals. The inter-orbital interaction between orbital c and orbitals a and b is denoted by V_p . Electrons in one orbital can pair with holes in the other two orbitals, and a competition exists between the two types of pairing. Here, $U_a = U_b = 4$, $U_c = 2$, $V = V_p = 5$. 1×2 - site CDMFT is used here.

of the other two orbitals, defining two distinct pairing channels (ab -, or ac - channel).

We first examine the case where all three orbitals are of d - electrons, thus large on-site U for all three orbitals shall be assumed. Here the influence of the additional d - hole orbital (orbital- c) is activated by gradually increasing its inter-orbital interaction strength, defined as $V_p \equiv V_{ac} = V_{bc}$ from zero. Simply speaking, when $V_p = 0$, the additional hole orbital- c is fully decoupled from the system, and when $V_p = V_{ab}$, both hole orbitals are equally coupled to the electron orbital. The corresponding evolution of the critical temperature T_c as a function of V_p is shown in Fig. 6(a), where $U_a = U_b = U_c = 4$, and $V_{ab} = 5$ is fixed. As V_p increased from zero, T_c initially remains nearly constant for $V_p \lesssim 2$, forming a plateau. Further increasing V_p then leads to significant suppression of T_c . At $V_p = 5$, namely, when inter-orbital interactions between three orbitals are equal, $V_{ab} = V_{bc} = V_{ac}$, the critical temperature is reduced to $T_c \approx 0.015$, a value slightly exceeding one-third of that at $V_p = 0$. This strong suppression of T_c upon introducing an additional pairing channel indicates that the competition between pairing channels, *i.e.*, pairing between ab -, or ac - channels, plays a crucial detrimental

tal role in the spontaneous formation of long-range excitonic order. This effect bears a conceptual resemblance to geometric frustration in magnetic systems, where competing magnetic couplings can prevent the establishment of long-range magnetic order, as seen in quantum spin liquids [73]. Here, an analogous “frustration” arises from the presence of multiple, near-degenerate electron-hole pairing channels, which suppresses the excitonic condensation. A key distinction, however, is that in the present case, long-range excitonic order persists even at the maximally frustrated point ($V_{ab} = V_{ac} = V_{bc}$), albeit with a significantly reduced T_c .

We then investigate the scenario with two d -orbitals and one p -orbital: a “strong U ” electron orbital (orbital- a) and a “strong U ” hole orbital (orbital- b) represent the d -orbitals, while a “weak U ” hole orbital (orbital- c) represents the p -orbital. For simplicity, all inter-orbital interactions V are set equal, $V_{ab} = V_{ac} = V_{bc}$. Fig. 6(b) presents the temperature dependence of the excitonic condensation order parameters $G_{mn} = \sum_{\sigma} \langle c_{im\sigma}^{\dagger} c_{in\sigma} \rangle$, for $(m, n) = (a, b), (a, c)$, for parameters $U_a = U_b = 4$, $U_c = 2$, and $V = 5$ in this system. The results reveal a remarkable orbital-selective electron-hole pairing phenomenon. Upon cooling, an excitonic order parameter between the $d-p$ orbitals (G_{ac}) emerges spontaneously below a critical temperature of $T_c \approx 0.032t$, and grows with further decreasing T . In contrast, the order parameter between two $d-d$ orbitals (G_{ab}) remains negligible at all temperatures, despite the symmetric inter-orbital attraction ($V_{ab} = V_{ac} = V_{bc}$). This orbital-selective excitonic condensation that prefers a $d-p$ condensation over a $d-d$ condensation likely stems from the effect of Hubbard U , which hinders inter-orbital exciton formation. The p -orbital, with its smaller U , is more susceptible to inter-orbital electron-hole binding than a d -orbital with a larger U . Consequently, the competition between multiple channels is resolved in favor of $d-p$ exciton condensation, resulting in paired states between $d-p$ orbitals and unpaired states between the $d-d$ orbitals.

Discussion and conclusion - In exciton insulator candidate comprising transition metal atoms, such as $\text{Ta}_2\text{Pd}_3\text{Te}_5$ and Ta_2NiSe_5 , electrons and holes are subject to multiple sources of Coulomb attractions. These multiple electron-hole binding routes effectively introduce a “frustration” effect that hinders the formation of exciton condensation. Notably, the on-site Hubbard interaction U , typically the largest energy scale in such systems, can facilitate the formation of local electron-hole pairs or local moments, thereby substantially suppressing the condensation temperature T_c . While our calculations are performed for semimetallic systems with finite carrier densities in the conduction and valence bands, our conclusions should, in principle, remain valid in the semiconductor limit. In actual semiconductors, although the valence band is completely filled and the

conduction band empty, orbital hybridization [19], from the local atomic orbital perspective, inevitably generates holes in the valence orbit and electrons in the conduction orbital, ensuring that the suppression of T_c by on-site Hubbard U persists. We underscore that theoretical studies on $\text{Ta}_2\text{Pd}_3\text{Te}_5$ predict a large exciton binding energy $\Delta \geq 0.6\text{eV}$ [19], while experimental measurements reveal a relatively low condensation temperature $T_c \sim 100\text{K}$ [9, 11], *i.e.* $k_B T_c \sim 0.01\text{eV}$. Our result may explain the apparent discrepancy between the large exciton binding energy and the low measured condensation temperature. It also offers insight into why exciton insulators remain so difficult to detect experimentally, despite the fact that exciton binding energies can be on the order of $\sim 1\text{eV}$ in low-dimensional materials [61–63].

In summary, we have systematically investigated spatially indirect exciton condensation in the two-dimensional Hubbard model on a triangular lattice using dynamical mean-field theory. Our results show that the critical temperature T_c for exciton condensation can be strongly suppressed by intra-orbital Coulomb repulsion U of the d -orbitals. We uncover a remarkable contrast in the density dependence of T_c between $U = 0$ and $U \neq 0$ cases. Extending our analysis to a three-orbital model, we further identify an orbital-selective electron-hole pairing state. These findings indicate that competition among multiple pairing channels in exciton insulator systems can significantly reduce T_c even in the presence of a large exciton binding energy. Our results illuminate the intricate interplay among Coulomb interactions, carrier density, and orbital degrees of freedom, providing valuable theoretical insights into the behavior of excitonic insulators in strongly correlated materials.

Acknowledgment We thank Shi-Cong Mo and Sheng Chen for useful discussions. This work is supported by the National Natural Science Foundation of China (Grants No.12274472, No.12494594). We also thank the support from the Research Center for Magneto-electric Physics of Guangdong Province (Grants No. 2024B0303390001) and Guangdong Provincial Quantum Science Strategic Initiative (Grant No. GDZX2401010).

* Corresponding author: wuwei69@mail.sysu.edu.cn

- [1] N. F. Mott, The transition to the metallic state, *Philosophical Magazine* **6**, 287 (1961).
- [2] J. M. Blatt, K. Böer, and W. Brandt, Bose-Einstein condensation of excitons, *Physical Review* **126**, 1691 (1962).
- [3] D. Jerome, T. Rice, and W. Kohn, Excitonic insulator, *Physical Review* **158**, 462 (1967).
- [4] J. Eisenstein and A. H. MacDonald, Bose-Einstein condensation of excitons in bilayer electron systems, *Nature* **432**, 691 (2004).
- [5] H. Cercellier, C. Monney, F. Clerc, C. Battaglia, L. Despont, M. G. Garnier, H. Beck, P. Aebi, L. Patthey, H. Berger, and L. Forró, Evidence for an excitonic in-

- sulator phase in 1T-TiSe₂, *Phys. Rev. Lett.* **99**, 146403 (2007).
- [6] Z. Jiang, Y. Li, W. Duan, and S. Zhang, Half-excitonic insulator: A single-spin Bose-Einstein condensate, *Phys. Rev. Lett.* **122**, 236402 (2019).
- [7] L. Ma, P. X. Nguyen, Z. Wang, Y. Zeng, K. Watanabe, T. Taniguchi, A. H. MacDonald, K. F. Mak, and J. Shan, Strongly correlated excitonic insulator in atomic double layers, *Nature* **598**, 585 (2021).
- [8] E. Baldini, A. Zong, D. Choi, C. Lee, M. H. Michael, L. Windgatter, I. I. Mazin, S. Latini, D. Azoury, B. Lv, *et al.*, The spontaneous symmetry breaking in Ta₂NiSe₅ is structural in nature, *Proceedings of the National Academy of Sciences* **120**, e2221688120 (2023).
- [9] P. Zhang, Y. Dong, D. Yan, B. Jiang, T. Yang, J. Li, Z. Guo, Y. Huang, Haobo, Q. Li, *et al.*, Spontaneous gap opening and potential excitonic states in an ideal dirac semimetal Ta₂Pd₃Te₅, *Physical Review X* **14**, 011047 (2024).
- [10] J. Huang, B. Jiang, J. Yao, D. Yan, X. Lei, J. Gao, Z. Guo, F. Jin, Y. Li, Z. Yuan, C. Chai, H. Sheng, M. Pan, F. Chen, J. Liu, S. Gao, G. Qu, B. Liu, Z. Jiang, Z. Liu, X. Ma, S. Zhou, Y. Huang, C. Yun, Q. Zhang, S. Li, S. Jin, H. Ding, J. Shen, D. Su, Y. Shi, Z. Wang, and T. Qian, Evidence for an excitonic insulator state in Ta₂Pd₃Te₅, *Phys. Rev. X* **14**, 011046 (2024).
- [11] M. S. Hossain, Z.-J. Cheng, Y.-X. Jiang, T. A. Cochran, S.-B. Zhang, H. Wu, X. Liu, X. Zheng, G. Cheng, B. Kim, *et al.*, Topological excitonic insulator with tunable momentum order, *Nature Physics* **21**, 1250 (2025).
- [12] Q. Gao, Y.-h. Chan, P. Jiao, H. Chen, S. Yin, K. Tangprapha, Y. Yang, X. Li, Z. Liu, D. Shen, *et al.*, Observation of possible excitonic charge density waves and metal-insulator transitions in atomically thin semimetals, *Nature Physics* **20**, 597 (2024).
- [13] Q. Wang, G. Xue, C. Ji, Y. Li, C. Li, L. Hou, X. Zheng, Q. Yu, C. Ma, X. Gan, *et al.*, Resonance tuning of localized excitons via a plasmonic nanocavity, *ACS nano* (2026).
- [14] Y. E. Lozovik and V. Yudson, A new mechanism for superconductivity: pairing between spatially separated electrons and holes, *Zh. Eksp. Teor. Fiz* **71**, 738 (1976).
- [15] F.-C. Wu, F. Xue, and A. H. MacDonald, Theory of two-dimensional spatially indirect equilibrium exciton condensates, *Phys. Rev. B* **92**, 165121 (2015).
- [16] Z. Jiang, Z. Liu, Y. Li, and W. Duan, Scaling universality between band gap and exciton binding energy of two-dimensional semiconductors, *Phys. Rev. Lett.* **118**, 266401 (2017).
- [17] M. Guan, D. Chen, Q. Chen, Y. Yao, and S. Meng, Coherent phonon assisted ultrafast order-parameter reversal and hidden metallic state in Ta₂NiSe₅, *Phys. Rev. Lett.* **131**, 256503 (2023).
- [18] Y. Shao and X. Dai, Electrical breakdown of excitonic insulators, *Phys. Rev. X* **14**, 021047 (2024).
- [19] J. Yao, H. Sheng, R. Zhang, R. Pang, J.-J. Zhou, Q. Wu, H. Weng, X. Dai, Z. Fang, and Z. Wang, Excitonic instability in Ta₂Pd₃Te₅ monolayer, *Chinese Physics Letters* **41**, 097101 (2024).
- [20] Y. Zeng, A. H. MacDonald, and N. Wei, Topological excitonic insulators in electron bilayers modulated by twisted hBN, *arXiv preprint arXiv:2509.11041* (2025).
- [21] Y. Xia, L. Shu, Y. Zhang, Y. Chen, L. Peng, J. Zhang, B. Li, H. Shao, Y. Cen, Z. Sui, *et al.*, Full-landscape condensation phases for long-lived excitons in 2d tellurium: Crystal-field splitting and finite-momentum excitons, *Advanced Functional Materials* **33**, 2303779 (2023).
- [22] G. Sreejith, J. D. Sau, and S. Das Sarma, Eliashberg theory for dynamical screening in bilayer exciton condensation, *Physical Review Letters* **133**, 056501 (2024).
- [23] S. Giuli, A. Amaricci, and M. Capone, Mott-enhanced exciton condensation in a hubbard bilayer, *Physical Review B* **108**, 165150 (2023).
- [24] J.-X. Zhu and A. Bishop, Exciton condensate modulation in electron-hole bilayers: A real-space visualization, *Physical Review B—Condensed Matter and Materials Physics* **81**, 115329 (2010).
- [25] J. Zhu and S. Das Sarma, Interaction and coherence in two-dimensional bilayers, *Physical Review B* **109**, 085129 (2024).
- [26] P. López Ríos, A. Perali, R. J. Needs, and D. Neilson, Evidence from quantum monte carlo simulations of large-gap superfluidity and BCS-BEC crossover in double electron-hole layers, *Physical Review Letters* **120**, 177701 (2018).
- [27] F. Nilsson and F. Aryasetiawan, Effects of dynamical screening on the BCS-BEC crossover in double bilayer graphene: Density functional theory for exciton bilayers, *Physical Review Materials* **5**, L050801 (2021).
- [28] B. H. Moon, A. Mondal, D. K. Efimkin, and Y. H. Lee, Exciton condensate in van der waals layered materials, *Nature Reviews Physics* , 1 (2025).
- [29] Q. Gao, Y.-h. Chan, Y. Wang, H. Zhang, P. Jinxi, S. Cui, Y. Yang, Z. Liu, D. Shen, Z. Sun, *et al.*, Evidence of high-temperature exciton condensation in a two-dimensional semimetal, *Nature Communications* **14**, 994 (2023).
- [30] Z. Wang, D. A. Rhodes, K. Watanabe, T. Taniguchi, J. C. Hone, J. Shan, and K. F. Mak, Evidence of high-temperature exciton condensation in two-dimensional atomic double layers, *Nature* **574**, 76 (2019).
- [31] S. Conti, A. Perali, A. R. Hamilton, M. V. Milošević, F. m. c. M. Peeters, and D. Neilson, Chester supersolid of spatially indirect excitons in double-layer semiconductor heterostructures, *Phys. Rev. Lett.* **130**, 057001 (2023).
- [32] Y.-H. Zhang, D. N. Sheng, and A. Vishwanath, SU(4) chiral spin liquid, exciton supersolid, and electric detection in moiré bilayers, *Phys. Rev. Lett.* **127**, 247701 (2021).
- [33] D. D. Dai and L. Fu, Strong-coupling phases of trions and excitons in electron-hole bilayers at commensurate densities, *Phys. Rev. Lett.* **132**, 196202 (2024).
- [34] X. Chen and J. Quinn, Excitonic charge-density-wave instability of spatially separated electron-hole layers in strong magnetic fields, *Physical review letters* **67**, 895 (1991).
- [35] Z. Bi and L. Fu, Excitonic density wave and spin-valley superfluid in bilayer transition metal dichalcogenide, *Nature communications* **12**, 642 (2021).
- [36] Y. Zeng, Z. Xia, R. Dery, K. Watanabe, T. Taniguchi, J. Shan, and K. F. Mak, Exciton density waves in Coulomb-coupled dual moiré lattices, *Nature Materials* **22**, 175 (2023).
- [37] S. Dong, Y. Chen, H. Qu, W.-K. Lou, and K. Chang, Topological exciton density wave in monolayer WSe₂, *Phys. Rev. Lett.* **134**, 066602 (2025).
- [38] R. Wang, T. A. Sedrakyanyan, B. Wang, L. Du, and R.-R. Du, Excitonic topological order in imbalanced electron-hole bilayers, *Nature* **619**, 57 (2023).
- [39] P. X. Nguyen, L. Ma, R. Chaturvedi, K. Watanabe,

- T. Taniguchi, J. Shan, and K. F. Mak, Perfect Coulomb drag in a dipolar excitonic insulator, *Science* **388**, 274 (2025).
- [40] R. Qi, A. Y. Joe, Z. Zhang, J. Xie, Q. Feng, Z. Lu, Z. Wang, T. Taniguchi, K. Watanabe, S. Tongay, *et al.*, Perfect Coulomb drag and exciton transport in an excitonic insulator, *Science* **388**, 278 (2025).
- [41] X. Zhu, P. B. Littlewood, M. S. Hybertsen, and T. M. Rice, Exciton condensate in semiconductor quantum well structures, *Phys. Rev. Lett.* **74**, 1633 (1995).
- [42] D. Snoke, Spontaneous bose coherence of excitons and polaritons, *Science* **298**, 1368 (2002).
- [43] K. Ulman and S. Y. Quek, Organic-2D material heterostructures: A promising platform for exciton condensation and multiplication, *Nano Letters* **21**, 8888 (2021).
- [44] E. C. Regan, D. Wang, E. Y. Paik, Y. Zeng, L. Zhang, J. Zhu, A. H. MacDonald, H. Deng, and F. Wang, Emerging exciton physics in transition metal dichalcogenide heterobilayers, *Nature Reviews Materials* **7**, 778 (2022).
- [45] D. Nandi, A. Finck, J. Eisenstein, L. Pfeiffer, and K. West, Exciton condensation and perfect Coulomb drag, *Nature* **488**, 481 (2012).
- [46] J. A. Seamons, C. P. Morath, J. L. Reno, and M. P. Lilly, Coulomb Drag in the Exciton Regime in Electron-Hole Bilayers, *Phys. Rev. Lett.* **102**, 026804 (2009).
- [47] A. Kogar, M. S. Rak, S. Vig, A. A. Husain, F. Flicker, Y. I. Joe, L. Venema, G. J. MacDougall, T. C. Chiang, E. Fradkin, *et al.*, Signatures of exciton condensation in a transition metal dichalcogenide, *Science* **358**, 1314 (2017).
- [48] Y. Ou, L. Chen, Z. Xin, Y. Ren, P. Yuan, Z. Wang, Y. Zhu, J. Chen, and Y. Zhang, Incoherence-to-coherence crossover observed in charge-density-wave material 1T-TiSe₂, *Nature Communications* **15**, 9202 (2024).
- [49] H. Yu, D. Yan, Z. Guo, Y. Zhou, X. Yang, P. Li, Z. Wang, X. Xiang, J. Li, X. Ma, R. Zhou, F. Hong, Y. Wuli, Y. Shi, J.-T. Wang, and X. Yu, Observation of emergent superconductivity in the topological insulator Ta₂Pd₃Te₅ via pressure manipulation, *Journal of the American Chemical Society* **146**, 3890 (2024), PMID: 38294957, <https://doi.org/10.1021/jacs.3c11364>.
- [50] S. Bae, A. Raghavan, I. Feldman, A. Kanigel, and V. Madhavan, Microscopic evidence of dominant excitonic instability in Ta₂NiSe₅, *arXiv preprint arXiv:2512.03011* (2025).
- [51] G. Mazza, M. Rösner, L. Windgätter, S. Latini, H. Hübener, A. J. Millis, A. Rubio, and A. Georges, Nature of symmetry breaking at the excitonic insulator transition: Ta₂NiSe₅, *Phys. Rev. Lett.* **124**, 197601 (2020).
- [52] Q. Liu, D. d. Wu, Z. Li, L. Shi, Z. Wang, S. Zhang, T. Lin, T. Hu, H. Tian, J. Li, *et al.*, Photoinduced multistage phase transitions in Ta₂NiSe₅, *Nature Communications* **12**, 2050 (2021).
- [53] K. Wei, Y. Luo, K. Watanabe, T. Taniguchi, Y. Guo, and X. Xi, Gate tuning of coupled electronic and structural phase transition in atomically thin Ta₂NiSe₅, *Nature Communications* **16**, 10999 (2025).
- [54] Z. Chen, C. Xu, C. Xie, W. Tang, Q. Liu, D. Wu, Q. Xu, T. Jiang, P. Zhu, X. Zou, *et al.*, Structural contribution to light-induced gap suppression in Ta₂NiSe₅, *Physical Review Letters* **135**, 096901 (2025).
- [55] K. Kim, H. Kim, J. Kim, C. Kwon, J. S. Kim, and B. Kim, Direct observation of excitonic instability in Ta₂NiSe₅, *Nature communications* **12**, 1969 (2021).
- [56] A. Kozlov and L. Maksimov, The metal-dielectric divalent crystal phase transition, *Sov. Phys. JETP* **21**, 790 (1965).
- [57] F. X. Bronold and H. Fehske, Possibility of an excitonic insulator at the semiconductor-semimetal transition, *Physical Review B—Condensed Matter and Materials Physics* **74**, 165107 (2006).
- [58] M. Fogler, L. Butov, and K. Novoselov, High-temperature superfluidity with indirect excitons in van der waals heterostructures, *Nature communications* **5**, 4555 (2014).
- [59] M. Combescot, R. Combescot, and F. Dubin, Bose-Einstein condensation and indirect excitons: a review, *Reports on Progress in Physics* **80**, 066501 (2017).
- [60] T. Kaneko and Y. Ohta, A new era of excitonic insulators, *Journal of the Physical Society of Japan* **94**, 012001 (2025).
- [61] H. Tang, L. Yin, G. I. Csonka, and A. Ruzsinszky, Exploring the exciton insulator state in 1T-TiSe₂ monolayer with advanced electronic structure methods, *Phys. Rev. B* **111**, L201401 (2025).
- [62] Y. Zhao, H. Qu, J. Zhao, L. Kang, and S. Zhou, One-dimensional excitonic insulator of M₆Te₆ (M = Mo, W) atomic wires, *Nano Letters* **25**, 1108 (2025).
- [63] D. Sun, Y. Xu, L.-A. Qin, Y. Dai, B. Huang, Z. Qian, R. Ahuja, and W. Wei, Breaking the synergy between the quasiparticle band gap and exciton binding energy, bright-dark exciton transition, and realization of the excitonic insulator state in quantum spin hall insulators, *Nano Letters* **25**, 18117 (2025).
- [64] H. R. Ramezani, E. Şaşıoğlu, H. Hadipour, H. R. Soleimani, C. Friedrich, S. Blügel, and I. Mertig, Non-conventional screening of Coulomb interaction in two-dimensional semiconductors and metals: A comprehensive constrained random phase approximation study of MX₂ (M = Mo, W, Nb, Ta; X = S, Se, Te), *Physical Review B* **109**, 125108 (2024).
- [65] A. Georges, G. Kotliar, W. Krauth, and M. J. Rozenberg, Dynamical mean-field theory of strongly correlated fermion systems and the limit of infinite dimensions, *Rev. Mod. Phys.* **68**, 13 (1996).
- [66] R. Blankenbecler, D. Scalapino, and R. Sugar, Monte carlo calculations of coupled boson-fermion systems. i, *Physical Review D* **24**, 2278 (1981).
- [67] P. Seth, I. Krivenko, M. Ferrero, and O. Parcollet, TRIQS/CTHYB: A continuous-time quantum monte carlo hybridisation expansion solver for quantum impurity problems, *Computer Physics Communications* **200**, 274 (2016).
- [68] O. Parcollet, M. Ferrero, T. Ayrál, H. Hafermann, I. Krivenko, L. Messio, and P. Seth, TRIQS: A toolbox for research on interacting quantum systems, *Computer Physics Communications* **196**, 398–415 (2015).
- [69] X. Ma, G. Wang, H. Mao, Z. Yuan, T. Yu, R. Liu, Y. Peng, P. Zheng, and Z. Yin, Ta₂NiSe₅: A candidate topological excitonic insulator with multiple band inversions, *Phys. Rev. B* **105**, 035138 (2022).
- [70] E. Cappelluti, R. Roldán, J. Silva-Guillén, P. Ordejón, and F. Guinea, Tight-binding model and direct-gap/indirect-gap transition in single-layer and multilayer MoS₂, *Physical Review B—Condensed Matter and Materials Physics* **88**, 075409 (2013).

- [71] Z. Y. Zhu, Y. C. Cheng, and U. Schwingenschlögl, Giant spin-orbit-induced spin splitting in two-dimensional transition-metal dichalcogenide semiconductors, [Phys. Rev. B **84**, 153402 \(2011\)](#).
- [72] G.-B. Liu, W.-Y. Shan, Y. Yao, W. Yao, and D. Xiao, Three-band tight-binding model for monolayers of group-VIB transition metal dichalcogenides, [Physical Review B—Condensed Matter and Materials Physics **88**, 085433 \(2013\)](#).
- [73] Y. Zhou, K. Kanoda, and T.-K. Ng, Quantum spin liquid states, [Reviews of Modern Physics **89**, 025003 \(2017\)](#).